Ultrasound in Med. & Biol. Vol. 14, No. 8, pp. 735–742, 1988
Printed in the U.S.A.

0301-5629/88 $3.00 + .00

●*Original Contribution*

EXPOSURE LEVELS FOR ULTRASONIC CAVITATION IN THE MOUSE NEONATE

C. S. LEE AND L. A. FRIZZELL
Bioacoustics Research Laboratory, Department of Electrical and Computer Engineering, University of Illinois, 1406 West Green Street, Urbana, Illinois 61801†

(*Received* 24 *September* 1987; *in final form* 9 *May* 1988)

Abstract—The levels for hind limb paralysis from 1 MHz, continuous wave, unfocused ultrasound in the neonatal mouse were determined at 1 and 16 bars hydrostatic pressure and at 10 and 37°C. Above a specific intensity level at each temperature, the exposure duration for paralysis of 50% of specimens exposed (t_{50}) was found to be greater at 16 bars than at 1 bar suggesting a threshold for cavitational involvement. Using these results, the intensity thresholds for cavitation were found to be in the ranges of 120–150 W/cm² and 53–74 W/cm² at 10°C and 37°C, respectively. This temperature dependence is consistent with a cavitation mechanism. In addition, the t_{50} at 289 W/cm² and 10°C was measured as a function of hydrostatic pressure and showed that cavitation was suppressed at hydrostatic pressures above approximately 10 bars. This result and the intensity threshold for cavitation at 1 bar and 10°C yielded similar values for the threshold negative total pressure for cavitation in the neonatal mouse.

Key Words: **Ultrasound, Bioeffects, Cavitation, Mouse neonate, Hind limb paralysis.**

INTRODUCTION

Ultrasound is known to induce biological effects by thermal and nonthermal mechanisms. Of the several nonthermal mechanisms which may be important, cavitation has been shown to be the cause of many effects *in vitro* (Ciaravino et al., 1981), in plants (Carstensen et al., 1979), and in fruitflies (Child et al., 1981). Additionally, Apfel (1982, 1986) and Flynn (1982) have shown theoretically that cavitation can occur from diagnostic-like microsecond pulses of ultrasound in water. ter Haar and Daniels (1986) have shown that bubbles can be caused to grow by ultrasound irradiation of the guinea pig hind limb at less than 1 W/cm², demonstrating the existence of nuclei in mammals. Yet it has been shown previously (Fry et al., 1971; Dunn and Fry, 1971; Lele et al., 1973; Lele, 1987; Frizzell, 1988) that intensities on the order of 1500 W/cm² are needed to produce transient cavitation-type damage to mammalian brain and liver by focused ultrasound. Thus the role of cavitation in the production of biological effects in mammals needs further investigation.

The mouse neonate has been a useful model for the determination of the exposure conditions for hind limb paralysis associated with exposure to unfocused ultrasound (Dunn, 1958; Frizzell et al., 1983). Frizzell et al. (1983) reported that at 1 MHz and 10°C, at intensities of 144 W/cm² and lower, there was no change in the exposure duration for paralysis of 50% of specimens exposed (t_{50}) between exposures at 1 and 16 bars (1 bar = 100 kPa) hydrostatic pressure. Conversely, at 289 W/cm² the t_{50} nearly doubled with the increase in pressure. Since increased pressure tends to suppress cavitational effects (Flynn, 1964; ter Haar et al., 1982; Lele, 1987), this was evidence for cavitation involvement at 289 W/cm² at 1 bar hydrostatic pressure. Additionally, Frizzell and Lee (1986) reported that the minimum intensity for cavitational involvement in the hind limb paralysis is lower at 37°C than at 10°C.

In this study, the levels for hind limb paralysis from 1 MHz, continuous wave, unfocused ultrasound in the neonatal mouse were determined at 1 and 16 bars hydrostatic pressure and at 10°C and 37°C. The t_{50} at 289 W/cm² and 10°C was measured as a function of hydrostatic pressure. Using these results, the threshold exposure conditions for cavitational involvement at 10 and 37°C were determined.

† Address all correspondence to: Leon A. Frizzell.

METHODS AND PROCEDURE

The details of the equipment, irradiation procedure, and data analysis have been reported previously (Frizzell et al., 1983) and are only summarized here. The specimens were ICR [Hap: (ICR)BR Harlan Industries] Swiss white laboratory mouse neonates harvested within 24 hours of birth (mean weight 1.61 g, standard deviation 0.06 g). Only those animals weighing within one standard deviation of the mean were used for this study. The neonates were anesthetized by lowering their body temperature to about 10°C via placement on ice for irradiation at 10°C, or by intramuscular injections, at the gluteal regions, of ketamine hydrochloride and xylazine, each at a dosage of 25 mg/kg, for irradiation at 37°C and for several data points at 10°C. For three sets of experiments at 37°C, halothane gas was used as the anesthetic.

After anesthetization the specimen was mounted in a specimen holder assembly, and the dorsal skin overlying the lumbar vertebral region was surgically removed. The specimen was aligned using an optical microscope and a high-intensity backlight so that, upon placing the holder assembly in the irradiation chamber (see Fig. 1), the ultrasound beam was centered on the third lumbar vertebral region on the dorsal side of the animal. The irradiation chamber contained degassed Ringer's solution coupling medium maintained at the desired temperature within 0.1°C. The specimen was located in the far field of the 1 MHz unfocused quartz source, where the trans-

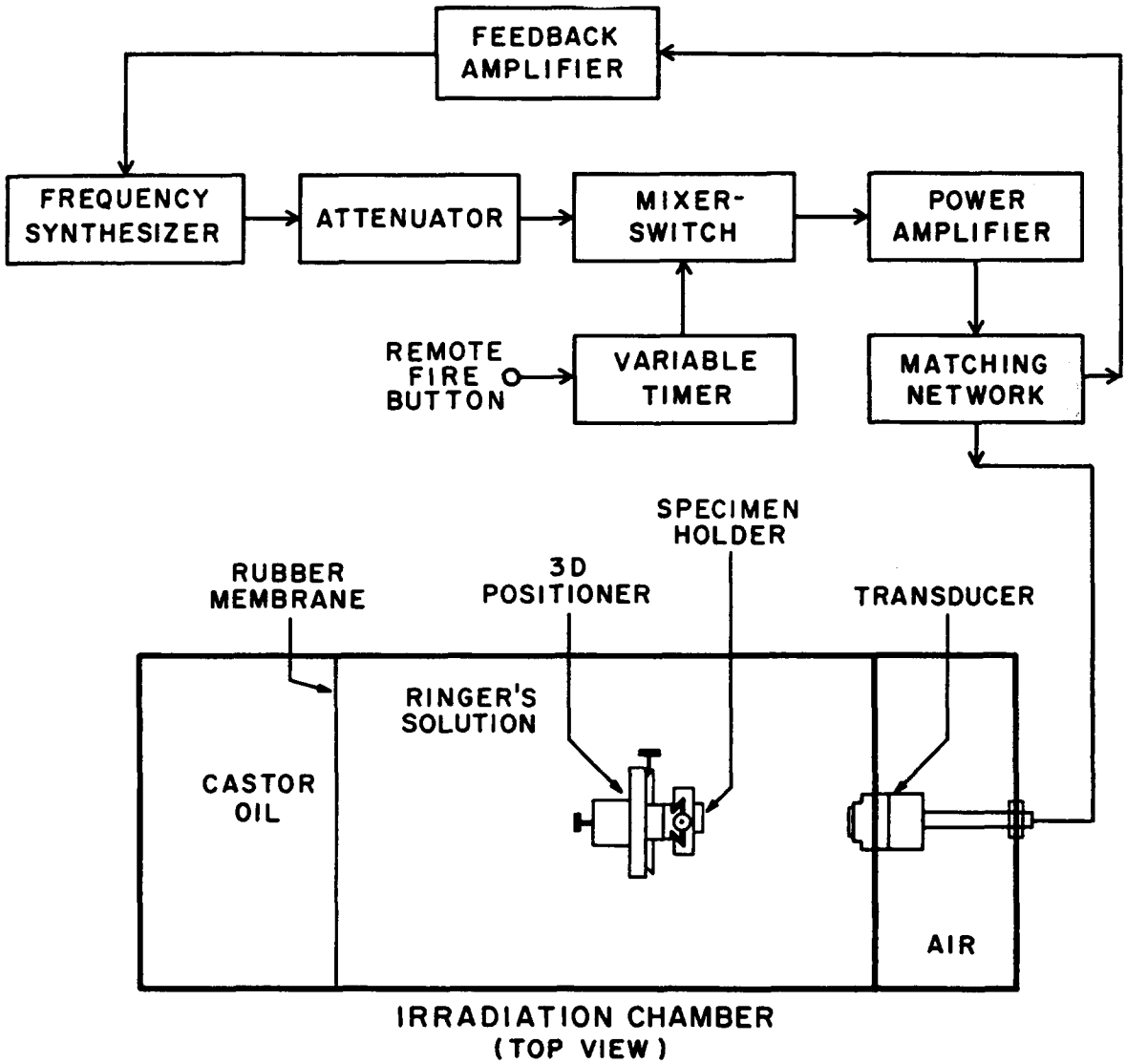

Fig. 1. Block diagram of the system electronics and irradiation chamber.

verse width of the ultrasound beam, to points of 95% of peak intensity, was approximately 3 mm.

In this study the intensity reported is the spatial peak intensity, but the intensity was well within 5% of the peak over the entire third lumbar region of the neonate as indicated by the beam width reported above. The *in situ* intensity is not reported because the path to the ventral side of the spinal cord, where the motor neurons are located, contains more than one tissue and there is some uncertainty in their thickness. However, an estimate of the maximum effect of attenuation yields a value for the *in situ* intensity 8% lower than the incident intensity. This calculation assumed a cartilage layer of thickness 0.05 cm, representing the dorsal portion of the spinal column which is minimally ossified, and a 0.1 cm depth of spinal cord. Recall that the skin was removed prior to irradiation. The corresponding attenuation coefficients used were 0.58 cm^{-1} (Dussik and Fritch, 1956) and 0.1 (Dunn and Brady, 1974). Since the value for cartilage increases with age (Dussik and Fritch, 1956), it is likely that the attenuation in the cartilage of the dorsal surface of the spinal column in the neonate is less than used for this calculation. Thus, the effects of linear attenuation should result in *in situ* intensities well within 8% of the reported intensities. However, it is also expected that harmonic generation due to nonlinear propagation will occur at the higher intensities used in this study, which means that some of the energy incident on the specimen will be in the harmonics of 1 MHz. This will result in increased absorption and a decreased amplitude at 1 MHz.

The electronics for driving the transducer consisted of a Wavetek model 3006 synthesized signal generator with attenuator, whose output was connected to a mixer controlled by an accurate counter to pass the signal for the desired exposure duration (see Fig. 1). The gated rf pulse was amplified by a 500-W Electronic Navigation Industries model A-500 wideband amplifier and fed through a matching and feedback network to the transducer. The feedback signal was amplified and used to control the amplitude of the signal from the signal generator to maintain the necessary voltage on the quartz transducer to produce the desired sound intensity at the specimen.

For the irradiations performed at atmospheric pressure, the specimen was irradiated approximately 5 min after placement in the irradiation chamber. This allowed ample time for the temperature of the mouse neonate to reach equilibrium. At equilibrium the core body temperature of the specimen, which was measured by embedding a small thermocouple probe in the abdomen of several specimens, was 10.2 $\pm$ 0.1°C and 37.1 $\pm$ 0.1°C when the temperature of the Ringer's coupling medium was 10°C and 37°C, respectively. After irradiation the specimen was removed from the irradiation chamber and allowed to recover from the anesthetic. For those animals anesthetized by cooling, full recovery was achieved after a 15 min warming period at room temperature. For those animals anesthetized with intramuscular injections of ketamine hydrochloride and xylazine, full recovery was achieved at approximately 3–4 h at room temperature. Animals anesthetized by inhalation of halothane gas recovered fully in about 20 min. When the irradiations were performed above atmospheric pressure, particularly at 16 bars, the specimen was irradiated approximately 15 min after placement in the irradiation chamber. It took about 5 min to seal the irradiation chamber and 10 min to pressurize the chamber using compressed air. After the irradiation, the chamber was decompressed slowly for 15 min. The recovery time for animals irradiated under hyperbaric conditions was similar to that for animals irradiated at atmospheric pressure. Sham irradiation experiments were performed at a hydrostatic pressure of 16 bars at both 10°C and 37°C, each with 20 animals. No functional changes or other adverse effects were observed at either temperature up to 4 h post-sham irradiation.

Those animals anesthetized by cooling were examined initially at a minimum of 4 min, and again at 15 min, post-irradiation for hind limb paralysis (Frizzell et al., 1983). Those animals anesthetized by halothane were examined approximately 20 min post-irradiation, and those anesthetized by ketamine hydrochloride and xylazine were examined approximately 4 h post-irradiation. Overall the results appeared to show little difference with time of examination. The examination was achieved by gently stimulating the hind feet, tail, or belly of the neonate with a small surgical forceps. If no functional alteration had occurred, the animal responded with a strong reflexive movement of the hind limbs. Paralyzed specimens exhibited no reflexive response of the hind limbs.

At the desired temperature and pressure, approximately 20 mouse neonates were irradiated at a specified intensity and exposure duration. This procedure was repeated for five or six different exposure durations at a common intensity, and the percentage of the specimens with hind limb paralysis was determined at each exposure duration. These results were plotted as the percentage of specimens paralyzed versus the inverse of the exposure duration, and a

probit analysis (Finney, 1971) was performed to determine the exposure duration for 10, 50, and 90% occurrence of paralysis at the specified intensity level (see Fig. 2). The combination of the intensity and the exposure duration for paralysis in 50% of specimens exposed specifies the effective dose 50%, ED_{50}, exposure conditions. Additional details of this method can be found in a previous publication (Frizzell et al., 1983).

RESULTS AND DISCUSSION

The ED_{50} ultrasonic exposure conditions for hind limb paralysis in the mouse neonate were determined at 1 and 16 bars hydrostatic pressure and at both 10° and 37°C temperature for the intensity range of 45 to 289 W/cm^2 (see Table 1). In order to fully assess the effect of the different methods of anesthesia, the ED_{50} ultrasonic exposure conditions were determined using the different aforementioned methods of anesthesia for several intensity levels at atmospheric pressure and at both 10 and 37°C (see Table 1). The results appear to be independent of the methods of anesthesia employed in this study.

The probit fit to the sigmoid curve for percentage of specimens paralyzed versus the inverse of exposure duration (see Fig. 2) yielded a 95% confidence interval of less than 1% in all but one case. To get a better determination of the variability associated with these measurements, the t_{50} at 86 W/cm^2, 37°C and 1 bar was determined five separate times (see Table 2). Four of the experiments for this study were performed using ketamine HCl and xylazine as the anesthetic agent, and one experiment was performed using halothane. As noted above, the results appear to be independent of the method of anesthesia. The mean and the standard error of these five sets of experiments were 0.66 s and 0.005 s, respectively, for a coefficient of variation of 0.8%. Since the determination of one t_{50} value at 1 bar ambient pressure takes approximately two to three weeks, it was not feasible to perform multiple determinations at all intensities, temperatures, and pressures. However, on occasions when new personnel began performing the experiments, they were required to repeat a previous measurement. Repetition involving different personnel and anesthetics showed agreement within three percent (Frizzell and Lee, 1986).

The ED_{50} data from Table 1 are plotted as intensity versus exposure duration in Fig. 3. Comparison of the data at 1 and 16 bars hydrostatic pressure shows that the results are independent of pressure at low intensities, but above a certain intensity level the ED_{50} ultrasonic exposure conditions are greater at 16

Table 1. Exposure duration t_{10}, t_{50}, and t_{90} in seconds for ED_{10}, ED_{50}, and ED_{90} exposure conditions, respectively, at 1 MHz. I is the ultrasonic intensity in W/cm^2, P is the hydrostatic pressure in bars, and T is the ambient temperature. Abbreviations CO, KX, and HT denote anesthesia induction by cooling on ice, ketamine HCl and xylazine, and halothane, respectively.

I	P	Anesthesia	t_{10}	t_{50}	t_{90}
T = 10°C					
45	1	CO	25.00	51.00	—
86	1	CO	3.40	5.00	9.40
86	1	KX	3.60	5.00	8.60
86	16	CO	3.20	4.90	9.70
105	1	CO	2.00	2.60	3.50
122	1	CO	1.40	1.50	1.70
144	1	CO	0.84	0.97	1.10
144	1	KX	0.85	0.99	1.20
144	16	CO	0.85	0.97	1.10
192	1	CO	0.36	0.44	0.58
192	1	KX	0.36	0.46	0.61
192	16	CO	0.44	0.63	1.10
256	1	CO	0.23	0.30	0.45
289	1	CO	0.20	0.26	0.37
289	16	CO	0.29	0.50	1.50
T = 37°C					
45	1	KX	3.20	5.00	11.00
45	1	HT	3.50	5.00	9.40
45	16	KX	3.10	4.70	10.00
86	1	KX	0.53	0.67	0.89
86	1	HT	0.53	0.65	0.84
86	16	KX	0.60	0.77	1.10
105	1	KX	0.26	0.35	0.50
105	1	HT	0.27	0.35	0.52
105	16	KX	0.36	0.50	0.82
122	1	KX	0.21	0.27	0.37
122	16	KX	0.25	0.37	0.73

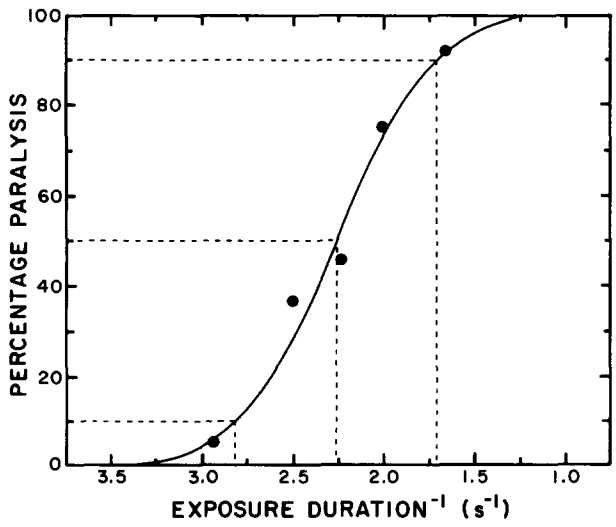

Fig. 2. Plot of percentage of specimens paralyzed versus t^{-1} at 192 W/cm^2 and 1 MHz in 10°C Ringer's solution. The solid line is derived from the probit analysis. The dashed lines indicate the 10, 50, and 90% paralysis conditions.

Table 2. Exposure durations t_{10}, t_{50}, and t_{90} in seconds for ED_{10}, ED_{50}, and ED_{90} exposure conditions, respectively, at 86 W/cm^2, 37°C, and a hydrostatic pressure of 1 bar.

Description	Anesthetic	t_{10}	t_{50}	t_{90}
Exp. 1	ketamine HCl + xylazine	0.53	0.67	0.89
Exp. 2	ketamine HCl + xylazine	0.51	0.66	0.92
Exp. 3	ketamine HCl + xylazine	0.53	0.68	0.95
Exp. 4	ketamine HCl + xylazine	0.53	0.66	0.88
Exp. 1–4				
mean		0.53	0.67	0.91
standard error		0.0050	0.0048	0.016
Exp. 5	halothane	0.53	0.65	0.84
Exp. 1–5				
mean		0.53	0.66	0.90
standard error		0.0040	0.0049	0.019

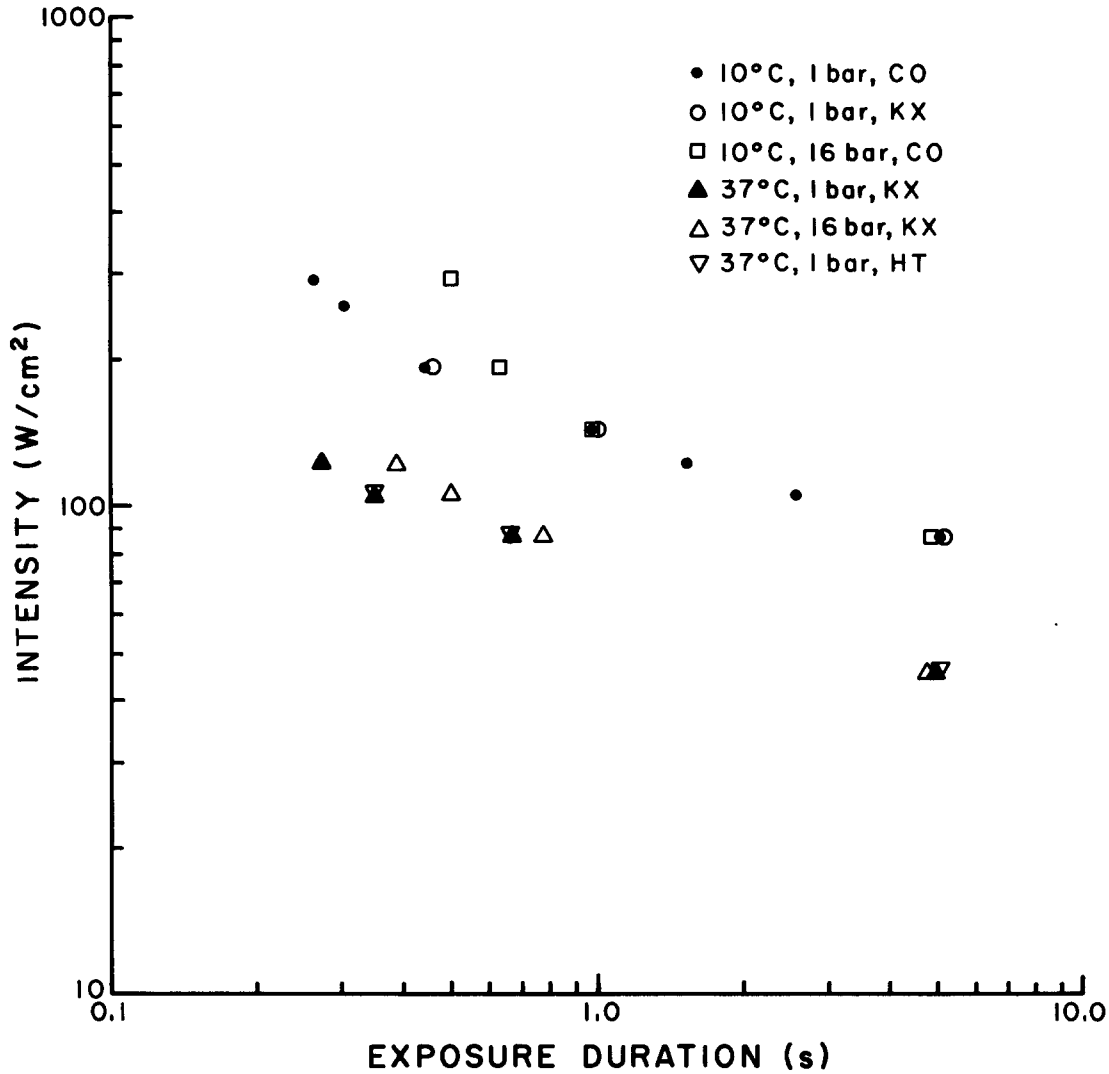

Fig. 3. The ED_{50} exposure conditions for hind limb paralysis in the mouse neonate at 1 MHz in Ringer's solution, *viz.*, intensity versus exposure duration. Abbreviations CO, KX, and HT denote anesthesia induction by cooling, ketamine HCl and xylazine, and halothane, respectively.

Table 3. Polynomial regression model by the method of least squares for the different sets of data given in Table 1. The fitted model is of the form: $\log t_n$ = Intercept − A $\log I$ + B$(\log I)^2$, where I is the ultrasonic intensity, t_n is the exposure duration, and n is the percentage of specimens paralyzed. T is the ambient temperature and P is the hydrostatic pressure.

T (°C)	P (bars)	n	Intercept	A	B	F† value	Intersection Pt. I (W/cm²)	Intersection Pt. t_n (s)
10	1	50	13.3	9.78	1.67	1700	120	1.7
10	16	50	16.5	13.2	2.60	520		
10	1	10	9.53	6.43	0.92	990	120	1.4
10	16	10	11.4	8.45	1.46	740		
37	1	50	10.2	7.92	1.33	300	53	2.8
37	16	50	10.5	8.60	1.62	50000		
37	1	10	7.04	4.88	0.56	108	49	2.5
37	16	10	4.80	2.69	0.05	25000		

† The F value is an indicator of how well the curve fits the data. The larger the F value, the better the fit.

bars than at 1 bar. Assuming that the standard error associated with each t_{50} value is not greater than 3% of the mean, then the differences in the observed t_{50} at 1 bar and 16 bars hydrostatic pressure at intensity levels of 192 W/cm² and 289 W/cm² at 10°C and at intensity levels of 86 W/cm², 105 W/cm², and 122 W/cm² at 37°C are all statistically significant at $p < 0.001$. Since an increased hydrostatic pressure tends to suppress cavitation (Flynn, 1964; ter Haar et al., 1982; Lele, 1987), cavitational involvement is indicated for exposures at 1 bar for exposure levels which show an effect of hydrostatic pressure on the ED_{50}. The results also show that with an elevation in the temperature, cavitation appears to be involved at a lower intensity level. This temperature dependence is consistent with a cavitation mechanism (Flynn, 1964; Crum, 1979).

Visual inspection of Fig. 3 would suggest that the threshold intensities for cavitational involvement are approximately 150 W/cm² at 10°C and 60 W/cm² at 37°C. In order to determine precisely the threshold intensity for cavitational involvement at both temperatures, the data of Table 1, and Fig. 3, for each temperature and pressure were fit to a second-order polynomial curve minimizing least-square error. Similar procedures were performed for the corresponding ED_{10} exposure conditions listed in Table 1. The results and statistical data are listed in Table 3, and the ED_{50} data at 10° and 37°C are plotted in Figs. 4 and 5, respectively. The maximum intensity for intersection of the 1 and 16 bar curves yielded intensity thresholds for cavitation at 120 W/cm² and 53 W/cm² at 10 and 37°C, respectively. As seen in Table 3, the results based on the ED_{10} exposure conditions are similar. These values are lower than expected based on the visual inspection of Fig. 3. However, when a 3% error is added to the t_{50} values, the highest intersection point is 150 W/cm² and 0.92 s at 10°C and 74 W/cm² and 1.1 s at 37°C. Thus, it seems appropriate to consider that the threshold for cavitational involvement falls in the ranges of 120–150 W/cm² at 1.7–0.92 s exposure duration at 10°C and 53–74 W/cm² at 2.8–1.1 s exposure duration at 37°C. Finally, it should be understood that the particular polynomial function used to generate the data of Table 3 was chosen because it provided an excellent fit to the data and does not imply an underlying model which explains the shapes of the curves.

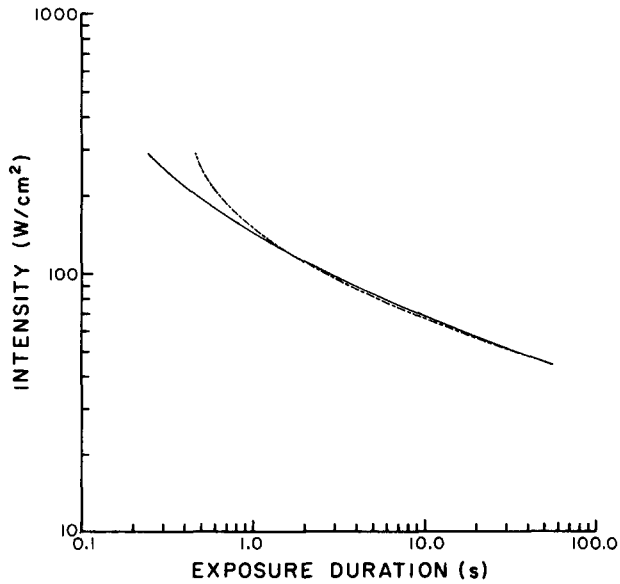

Fig. 4. Plot of intensity versus exposure duration curves generated by a polynomial regression fit to the ED_{50} exposure conditions at 10°C. The solid and dashed curves represent exposure at 1 bar and 16 bars hydrostatic pressure, respectively.

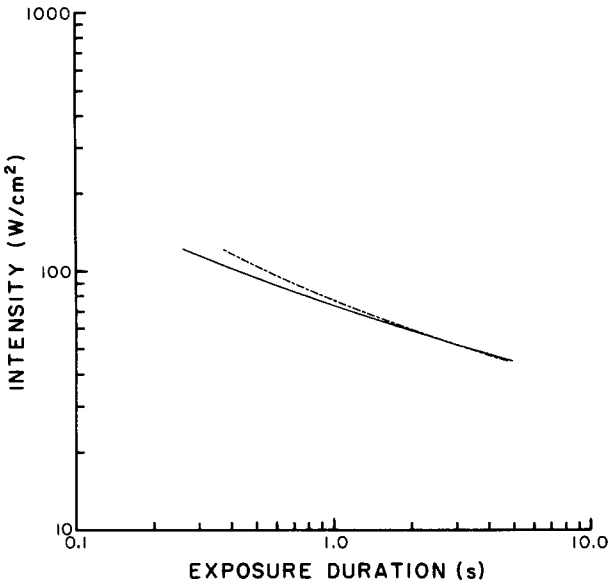

Fig. 5. Plot of intensity versus exposure duration curves generated by a polynomial regression fit to the ED_{50} exposure conditions at 37°C. The solid and dashed curves represent exposure at 1 bar and 16 bars hydrostatic pressure, respectively.

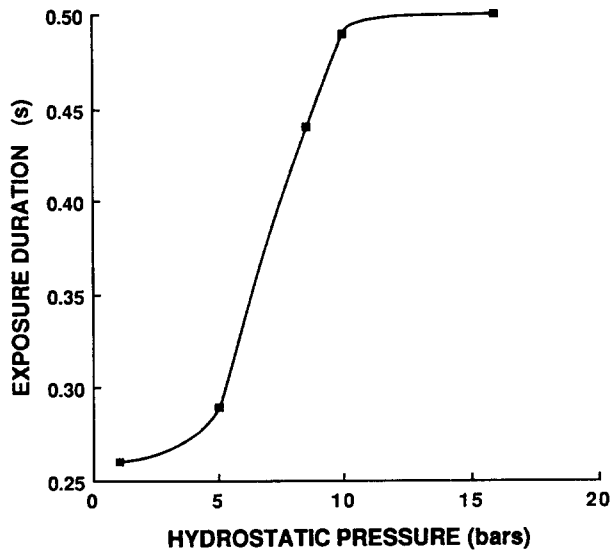

Fig. 6. Plot of the exposure duration for paralysis of 50% of specimens, t_{50}, versus hydrostatic pressure at an intensity of 289 W/cm² and at 10°C.

The t_{50} at 10°C and at 289 W/cm² was determined as a function of hydrostatic pressure over the range from 1 to 16 bars. The results are listed in Table 4 and are plotted in Fig. 6. From the plot in Fig. 6, it can be seen clearly that the t_{50} essentially reaches an asymptotic value of 0.50 s when the hydrostatic pressure is increased beyond approximately 10 bars. This indicates that the effect of cavitation is suppressed at pressures greater than this threshold value. These results can be compared to the results in Table 3 in the following way.

For a traveling plane acoustic wave, the time averaged intensity I can be expressed as

$$I = \frac{P_a^2}{2\rho c}, \tag{1}$$

where P_a is the acoustic pressure amplitude and ρc is the product of density and speed of sound of the medium. In general, transient cavitation does not occur in a liquid medium unless the maximum negative value of the total pressure is lower than a certain threshold value P_{th}, where the total pressure P_t is given by

$$P_t = P_a \cos \omega t + P_h, \tag{2}$$

where P_h is the hydrostatic pressure and ω is the angular frequency. If the intensity threshold for cavitation is taken as being in the range of 120–150 W/cm² at 10°C and 1 bar hydrostatic pressure, then, using equations (1) and (2), P_{th} is calculated to be in the range of −18 to −20 bars, where the acoustic impedance ρc for the Ringer's coupling medium at 10°C was taken as 1.47×10^6 MKS rayls. For intensities above this threshold range, suppression of cavitation would occur if the hydrostatic pressure is large enough such that P_t is always greater than P_{th}. Based on the data of Table 4 and Fig. 6, cavitation was suppressed at 289 W/cm² when the hydrostatic pressure exceeded approximately 10 bars. This yields a P_{th} of approximately −19 bars which is in the range for P_{th} calculated above.

Table 4. Exposure duration t_{50} in seconds for ED_{50} exposure conditions at 289 W/cm² and 10°C. P is the hydrostatic pressure in bars.

P (bars)	t_{50} (s)
1	0.26
5	0.29
8.5	0.44
10	0.49
16	0.50

CONCLUSIONS

The results obtained in this study indicate that ultrasonically induced cavitation is involved in the production of hind limb paralysis of the mouse neonate at intensities above the range of 120–150 W/cm² at 10°C and above the range of 53–74 W/cm² at

37°C. This qualitative temperature dependence is as expected for cavitation phenomena.

The t_{50} was determined at 289 W/cm^2 and 10°C as a function of hydrostatic pressure showing that the t_{50} reaches an asymptotic value of 0.50 s when the hydrostatic pressure is increased beyond approximately 10 bars. Thus cavitation was suppressed when the hydrostatic pressure was greater than 10 bars.

An intensity of 120–150 W/cm^2 at 1 bar hydrostatic pressure and an intensity of 289 W/cm^2 at 10 bar hydrostatic pressure yield a maximum negative total pressure of −18 to −20 bars and −19 bars, respectively. Again, it should be noted that some harmonic generation is expected to occur due to nonlinear propagation in the coupling medium, which will reduce the amplitude of the 1 MHz signal. However, based on plane wave theory, the difference between this effect at 135 and 289 W/cm^2 is on the order of 10%. Thus, even considering nonlinear effects, both sets of experiments discussed above yield similar threshold maximum negative total pressures for cavitational involvement in the hind limb paralysis at 10°C. Since a cavitation threshold dependent upon the maximum negative total pressure is often indicative of transient cavitation, these results suggest that transient rather than stable cavitation may be responsible for the observed cavitational effects.

These threshold intensity levels are well below those determined for adult mammalian brain and liver (Fry et al., 1971; Dunn and Fry, 1971; Lele et al., 1973; Lele, 1987; Frizzell, 1988). Though the reason for this difference is not yet clear, these results are consistent with the lower intensity thresholds for cavitation observed by others for long exposure durations (Lehmann and Herrick, 1953; Martin et al., 1981; ter Haar et al., 1986). However, the threshold intensity levels reported here are well above the time-averaged intensities employed with diagnostic and diathermic ultrasonic systems. On the other hand, the effect of diagnosticlike short duration, repetitive pulses of ultrasound, where the temporal peak intensity may exceed these thresholds needs to be examined.

Acknowledgements—This study was supported in part by a grant from the National Institutes of Health.

The authors are especially thankful to R. S. Morimoto for his assistance in the irradiation procedures. The authors also wish to thank J. Cobb and B. McNeill for technical assistance, and R. Cicone for animal care.

REFERENCES

Apfel, R. E. Acoustic cavitation: A possible consequence of biomedical uses of ultrasound. Br. J. Cancer 45 (Suppl. V):140–146; 1982.

Apfel, R. E. Possibility of microcavitation from diagnostic ultrasound. IEEE Trans. Ultrasonics Ferroelectrics Freq. Control UFFC-33:139–142; 1986.

Carstensen, E. L.; Child, S. Z.; Law, W. K.; Horowitz, D. R.; Miller, M. W. Cavitation as a mechanism for the biological effects of ultrasound on plant roots. J. Acoust. Soc. Am. 66:1285–1291; 1979.

Child, S. Z.; Carstensen, E. L.; Lam, S. Effects of ultrasound on Drosophila: III. Exposure of larvae to low-temporal-average-intensity, pulsed ultrasound. Ultrasound in Med. & Biol. 7:167–173; 1981.

Ciaravino, V.; Flynn, H. G.; Miller, M. W. Pulsed enhancement of acoustic cavitation: A postulated model. Ultrasound in Med. & Biol. 7:159–166; 1981.

Crum, L. A. Tensile strength of water. Nature 278:148–149; 1979.

Dunn, F. Physical mechanisms of the action of intense ultrasound on tissue. J. Phys. Med. 37:148–151; 1958.

Dunn, F.; Brady, J. K. Ultrasonic absorption in biological media. Biofizika 18:1062–1072; 1973.

Dunn, F.; Fry, F. J. Ultrasonic threshold dosages for the mammalian central nervous system. IEEE Trans. Biomed. Eng. BME-18:253–256; 1971.

Dussik, K. T.; Fritch, D. J. Determination of sound attenuation and sound velocity in the structure constituting the joints, and of the ultrasonic field distribution within the joints of living tissues and anatomical preparations, both in normal and pathological conditions. Public Health Service, Natl. Inst. Health Project A454, Prog. Rep. (15 September, 1956).

Finney, D. J. Probit Analysis. London: Cambridge University Press; 1971.

Flynn, H. G. Physics of acoustic cavitation in liquids. In: Mason, W. P., ed., Physical Acoustics. New York: Academic Press; 1964:Vol. IB, Chap. 9.

Flynn, H. G. Generation of transient cavities in liquids by microsecond pulses of ultrasound. J. Acoust. Soc. Am. 72:1926–1932; 1982.

Frizzell, L. A. Threshold dosages for damage to mammalian liver by high intensity focused ultrasound. IEEE Trans. Ultrasonics, Ferroelectrics, and Frequency Control. UFFC-35:578–581; 1988.

Frizzell, L. A.; Lee, C. S. Exposure levels for ultrasonic cavitation in mammals. In: IEEE/Eighth Annual Conf. of the Engineering in Medicine and Biology Society Proc.; 1986:1026–1028.

Frizzell, L. A.; Lee, C. S.; Aschenbach, P. D.; Borrelli, M. J.; Morimoto, R. S.; Dunn, F. Involvement of ultrasonically induced cavitation in the production of hind limb paralysis of the mouse neonate. J. Acoust. Soc. Am. 74:1062–1065; 1983.

Fry, F. J.; Kossoff, G.; Eggleton, R. C.; Dunn, F. Threshold ultrasonic dosages for structural changes in mammalian brain. J. Acoust. Soc. Am. 48:1413–1417; 1971.

Lehmann, J. F.; Herrick, J. F. Biologic reactions to cavitation, a consideration for ultrasonic therapy. Arch. Phys. Med. 34:86–98; 1953.

Lele, P. P.; Senapati, N.; Hsu, W. L. Mechanisms of tissue—ultrasound interaction. In: deVlieger, M.; White, D. N.; McCready, V.R., eds., Ultrasonics in Medicine. Amsterdam: Excerpta Medica; 1973.

Lele, P. P. Effects of ultrasound on "solid" mammalian tissues and tumors *in vivo*. In: Repacholi, M. H.; Grandolfo, M.; Rindi, A., eds., Ultrasound. New York: Plenum Press; 1987.

Martin, C. J.; Gregory, D. W.; Hodgkiss, M. The effects of ultrasound *in vivo* on mouse liver in contact with an aqueous coupling medium. Ultrasound in Med. & Biol. 7:253–265; 1981.

ter Haar, G. R.; Daniels, S.; Morton, F. Evidence for acoustic cavitation *in vivo:* Thresholds for bubble formation with 0.75 MHz continuous wave and pulsed beams. IEEE Trans. Ultrasonics, Ferroelectrics, and Frequency Control UFFC-33: 162–164; 1986.

ter Haar, G. R.; Daniels, S.; Eastaugh, F. C.; Hill, C. R. Ultrasonically induced cavitation *in vivo*. Br. J. Cancer 45 (Suppl. V): 151–155; 1982.